Journal of Naval Architecture and Marine Engineering
December, 2023
http://dx.doi.org/10.3329/jname.v20i2.70314 *http://www.banglajol.info*

A NUMERICAL INVESTIGATION ON HYDRODYNAMIC INTERACTION COEFFICIENTS FOR TWO FREELY FLOATING BARGES OF TANDEM CONFIGURATION IN WAVES

M. T. Ali[1*] and G. Sobahani[2]

[1]Department of Naval Architecture and Marine Engineering, Bangladesh University of Engineering and Technology, Dhaka 1000, Bangladesh, [*]mtarequeali@name.buet.ac.bd

[2]Department of Naval Architecture and Marine Engineering, Bangladesh University of Engineering and Technology, Dhaka 1000, Bangladesh, gsobahani@name.buet.ac.bd

Abstract:

While installing offshore structures two or more structures are observed floating close to each other in waves. Consequently, the adjacent floating structures influence the fluid loading on each body. Due to radiated waves produced by the motion of adjoining floating structures and the wave reflection or, sheltering effect because of the presence of these nearby structures, the wave loading for the multi-body case will be quite different from that of a single-body case. Accurate computation of hydrodynamic interaction coefficients and hydrodynamic coefficients are vital for a multiple floating body case since the motion response prediction uses these parameters in solving the 6xN simultaneous equations (where N is the number of closely floating structures). The hydrodynamic interaction coefficients are investigated in this paper for two three-dimensional (3-D) structures floating closely in water. A commercial hydrodynamic software named Hydrostar (introduced by Bureau Veritas) which is based on linear three-dimensional potential theory is adopted for numerical simulations of the present problem. To validate the numerical results for hydrodynamic interaction coefficients, the present computation results are compared with the published results for a rectangular box and a vertical circular cylinder model floating closely in regular waves, and a satisfactory agreement is observed. Finally, numerical simulations are performed for two identical rectangular barges floating close to each other in the tandem arrangement in regular waves. During the computations, the gap between the floating barges is varied and the occurrence of hydrodynamic resonances in the gap is also examined. Lastly, considering the analysis for the multi-body case, a few conclusions are made.

Keywords: hydrodynamic interaction, potential flow theory, 3-D source distribution, floating barges.

NOMENCLATURE

a_{kj}	added mass coefficient in the k-th mode due to j-th mode of motion	X_j^2	motion of body 2 in the j-th mode
b_{kj}	damping coefficient in the k-th mode due to j-th mode of motion	***Greek symbols***	
F_k	wave-exciting force in the k-th mode	∇	displacement volume
g	acceleration due to gravity	ζ_a	incident wave amplitude
h	draft of the floating body	ρ	mass density of water
l	characteristics length	Φ	linear potential function of space and time
n_k^1	unit normal in the k-th mode for body 1	ϕ	linear potential function of space
n_k^2	unit normal in the k-th mode for body 2	ϕ_0	incident wave potential
o-xyx	coordinate system for the problem	ϕ_7	diffraction wave potential
p	pressure	ϕ_j^1	radiation potential of body 1 in the j-th mode
S	wetted surface area of the floating body	ϕ_j^2	radiation potential of body 2 in the j-th mode
t	time	ω	wave frequency
X_j^1	motion of body 1 in the j-th mode	ω_n	resonant frequency of n-th order

1813-8535 (Print), 2070-8998 (Online) Selected from papers presented at MARTEC 2022

1. Introduction

In offshore engineering, many applications exist where multiple floating structures are operating closely in harsh ocean environments. Examples of offshore operations involving two or more floating structures include mobile offshore drilling units, floating bridges, an array of floating offshore renewable energy platforms, offshore float-over installations, loading/offloading operations of LNG-FPSO, Shuttle Tanker-FPSO systems in side-by-side or tandem position, etc. As a matter of fact, for several bodies floating closely in waves, each body will experience an interaction effect due to the presence and movement of surrounding bodies, and their motion responses and wave forces will be influenced due to the variation in the separation distance (gap) between them. To avoid unfavorable responses and risk of collisions and to ensure the safety of mooring or, link systems for a multi-body floating system, it is essential to study the characteristics of hydrodynamic interaction coefficients of these floating bodies.

A number of researches have been conducted for multi-body problems focusing on hydrodynamic interactions between the floating bodies. Applying the source distribution technique, Ali (2021, 2020) investigated the hydrodynamic interaction coefficients for multiple floating bodies in regular waves. Chen et al. (2021) numerically examined the hydrodynamic interaction characteristics of several identical rectangular boxes in waves. Using both numerical and experimental techniques, Dinoi (2016) investigated some hydrodynamic aspects of a two-body floating system in a parallel arrangement. Ghafari et al. (2019) investigated the hydrodynamic interactions in the frequency domain and time domain for a Mono column type FPSO floating platform and a semi-submersible named Amirkabir in Caspian Sea Conditions. Li (2020) investigated the resonant characteristics and shielding effects of multi-bodies in parallel and nonparallel configurations for irregular waves. Sun et al. (2012) analyzed a float-over installation similar to a multi-body system and they studied the influence of diffraction by the large volume substructure. Van Oortmerssen (1979) solved the problem of hydrodynamic interactions for several floating bodies using linear 3-D diffraction theory.

This paper investigates the hydrodynamic interaction coefficients for two closely floating 3-D bodies in regular waves. A commercial hydrodynamic software named Hydrostar (introduced by Bureau Veritas) based on a linear 3-D potential theory is adopted for numerical simulations of the present problem. To validate the numerical results for hydrodynamic interaction coefficients, the present computation results are compared with the published results for a rectangular box and a vertical circular cylinder model floating closely in regular waves, and a satisfactory agreement is observed. Finally, numerical simulations are performed for two identical rectangular barges floating close to each other in the tandem arrangement in regular waves. During the computations, the gap between the floating barges is varied and the occurrence of hydrodynamic resonances in the gap is also examined. Lastly, considering the analysis for the multi-body case, a few conclusions are made.

2. Mathematical Formulation of the Problem

Consider two 3-D bodies−body 1 and body 2 of arbitrary shape, which are positioned nearby, oscillating sinusoidally with the waves in water of uniform depth. The motion amplitude of the floating bodies and waves is considered to be small, whereas the fluid is assumed to be incompressible, inviscid, and irrotational. To describe the motion response of the two bodies, as shown in Fig. 1, a space-fixed global coordinate system (o_0-$x_0y_0z_0$) and two local coordinate systems (o_1-$x_1y_1z_1$) and (o_2-$x_2y_2z_2$) that are fixed with respect to the mean position of body 1 and body 2 respectively are considered. For these coordinate systems, the origin is considered at the calm water surface with the z-axis positive in the vertically upward direction.

In the regular wave, Φ is a linear potential function of space and time, and it can be written as:

$$\Phi(x, y, z; t) = \mathrm{Re}[\phi(x, y, z).e^{-i\omega t}] \tag{1}$$

where the potential function $\phi(x, y, z)$ is a time-independent quantity and it can be separated into the incident, diffracted and radiation wave fields as:

$$\phi = -i\omega \left[(\phi_0 + \phi_7)\zeta_a + \sum_{j=1}^{6} X_j^1 \phi_j^1 + \sum_{j=1}^{6} X_j^2 \phi_j^2 \right] \tag{2}$$

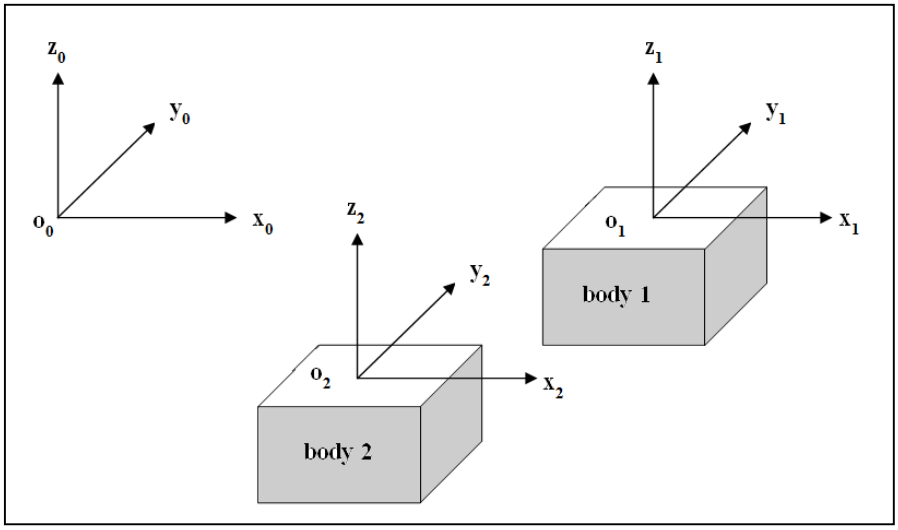

Fig. 1: Definition of coordinate system for multiple floating bodies

where ϕ_0 is the potential due to incident wave, ϕ_7 is the diffraction wave potential, ϕ_j^1 represent potentials due to the motion of body 1 in the j-th mode, ϕ_j^2 represent potentials due to the motion of body 2 in the j-th mode i.e., wave potentials due to radiation, X_j^1 is the motion of body 1 in j-th mode, X_j^2 is the motion of body 2 in j-th mode and ζ_a is the incident wave amplitude.

The individual potentials can be obtained from Laplace equation solutions and they need to satisfy linearized free surface condition, sea floor boundary condition, the wetted surface boundary condition for the floating bodies, and the boundary condition at infinity (Ali, 2020). Having solved the velocity potentials and applying the linearized Bernoulli's equation, the pressure on the structure at any point can be determined as follows:

$$p = -\rho\frac{\partial\Phi}{\partial t} = \rho\omega^2\left[(\phi_0+\phi_7)\zeta_a + \sum_{j=1}^{6} X_j^1\phi_j^1 + \sum_{j=1}^{6} X_j^2\phi_j^2\right]e^{-i\omega t} \tag{3}$$

Consequently, the hydrodynamic reactive forces can be written as:

$$F_k^1 = -\rho\omega^2 e^{-i\omega t}\sum_{j=1}^{6}\iint_{S^1}\left[\phi_j^1 X_j^1 + \phi_j^2 X_j^2\right]n_k^1\,dS \tag{4}$$

$$F_k^2 = -\rho\omega^2 e^{-i\omega t}\sum_{j=1}^{6}\iint_{S^2}\left[\phi_j^1 X_j^1 + \phi_j^2 X_j^2\right]n_k^2\,dS \tag{5}$$

The two components of reactive forces in phase with body velocity and body acceleration can be written as follows:

$$F_k = -\left(a_{kj}\ddot{X}_j + b_{kj}\dot{X}_j\right) = \left(\omega^2 a_{kj} + i\omega b_{kj}\right)X_j e^{-i\omega t} \tag{6}$$

where a_{kj} and b_{kj} are the added mass and damping coefficients respectively in the k-th mode due to j-th mode of motion. Now, equating the real and imaginary parts of the equation, the added mass, and damping coefficients due to own body motion and due to another body motion can be written as presented in Table 1:

Table1. Hydrodynamic interaction coefficients

Added mass coefficient	Damping coefficient
$a_{kj}^{12} = -\,\mathrm{Re}\left[\rho \iint_{S^1} \phi_j^2 n_k^1 \, dS\right]$	$b_{kj}^{12} = -\,\mathrm{Im}\left[\rho\omega \iint_{S^1} \phi_j^2 n_k^1 \, dS\right]$
$a_{kj}^{21} = -\,\mathrm{Re}\left[\rho \iint_{S^2} \phi_j^1 n_k^2 \, dS\right]$	$b_{kj}^{21} = -\,\mathrm{Im}\left[\rho\omega \iint_{S^2} \phi_j^1 n_k^2 \, dS\right]$

where a_{kj}^{mn} and b_{kj}^{mn} are the added mass and damping coefficients respectively in the k-th direction of m-th body due to j-th mode of motion of n-th body, and F_k^m is the wave-exciting force in the k-th mode of m-th body. According to Dmitrieva (1994) for multi-body motions, the hydrodynamic interaction coefficients satisfy the symmetry relationships, i.e.

$$a_{kj}^{12} = a_{jk}^{21} \tag{7}$$

$$b_{kj}^{12} = b_{jk}^{21} \tag{8}$$

3. Results and Discussion

A commercial hydrodynamic software named Hydrostar (introduced by Bureau Veritas) which is based on linear three-dimensional potential theory is adopted for numerical simulations of the present problem. The validation of the numerical results has been justified by comparing the present results with those of the published ones for the box and cylinder model closely floating in regular waves (Dmitrieva, 1994) and the agreement is quite satisfactory. Numerical simulations are further conducted for two closely floating identical rectangular barges in regular waves (Liang-yu. et al., 2014). During the computations of hydrodynamic interaction coefficients for tandem configurations, the gap width is varied to study their characteristics.

3.1 Rectangular box and vertical cylinder

To study the characteristics of hydrodynamic interaction coefficients for multiple floating bodies, numerical computation is initially carried out for a vertical circular cylinder (body 1) and a rectangular box (body 2) model freely floating in close proximity in regular waves. The vertical cylinder is 95.8 m in diameter and 30.0 m in the draft, whereas the rectangular box is 109.7 m in length, 101.4 m in breadth, and 30 m in draft. The wetted surfaces of the vertical cylinder (body 1) and the rectangular box (body 2) are divided into 1034 and 2240 panels respectively. The plan view for the box-cylinder model in side-by-side configuration is presented in Fig. 2.

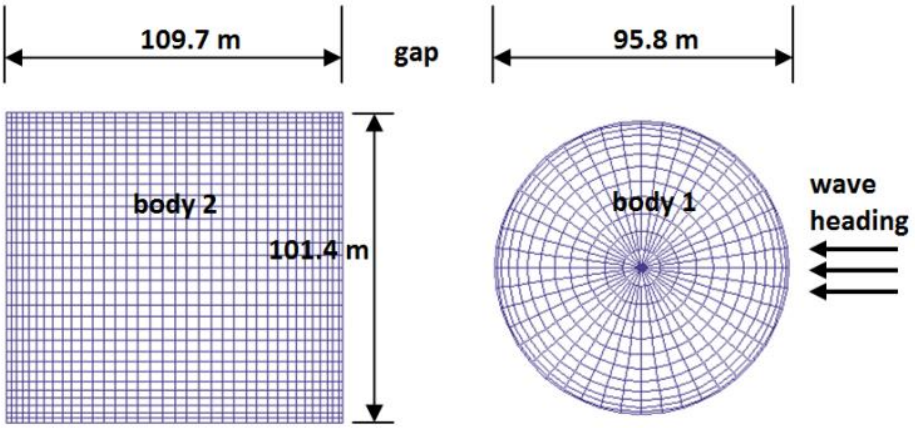

Fig. 2. The plan view for the floating rectangular box and vertical cylinder model in the side-by-side configuration

Numerical simulations for this multi-body model are conducted for the gap width of 50.0 m between the two bodies floating at the water of 220 m in depth. The hydrodynamic interaction coefficients of added mass and damping for surge and heave mode are non-dimensionalized by dividing with $\rho\zeta_a\nabla$ and $\rho\zeta_a\nabla\sqrt{g/l}$ respectively and the wave frequency is non-dimensionalized by multiplying with $\sqrt{l/g}$, where the characteristics length l is 101.4 m, ρ is the mass density of water, and ∇ is the volume displacement of the box.

Figs. 3(a) and 3(b) show the results of diagonal terms (surge-surge) for non-dimensional added mass $\left({}^{11}a_{11}^{*}\right)$ and damping $\left({}^{11}b_{11}^{*}\right)$ of the body 1 (vertical cylinder) in surge mode due to its own motion in surge mode. Similarly, Figs. 3(c) and 3(d) show the results of diagonal terms (heave-heave) for non-dimensional added mass $\left({}^{11}a_{33}^{*}\right)$ and damping $\left({}^{11}b_{33}^{*}\right)$ of the body 1 (vertical cylinder) in heave mode due to its own motion in heave mode. The present numerical results are compared with the numerical results of Dmitrieva and the experimental results of Oortmerssen (Dmitrieva, 1994). As can be seen from these figures, that the agreement between the calculated results are quite satisfactory, however the agreement with the experimental results present some deviations.

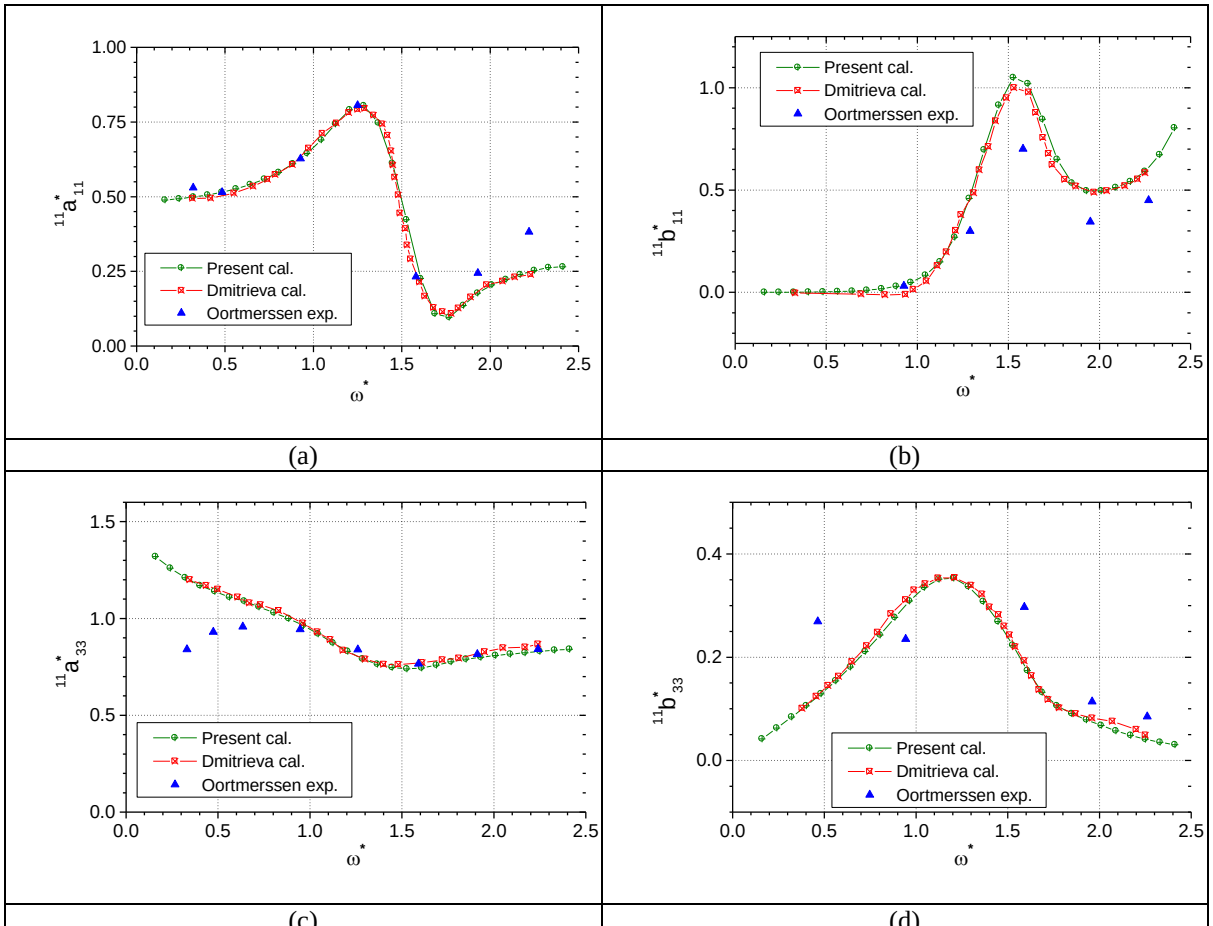

Fig. 3. Hydrodynamic interaction coefficients for floating rectangular box and vertical cylinder model in the side-by-side configuration

Figs. 4(a) and 4(b) show the results of diagonal terms (surge-surge) for non-dimensional added mass $\left({}^{22}a_{11}^{*}\right)$ and damping $\left({}^{22}b_{11}^{*}\right)$ of the body 2 (rectangular box) in surge mode due to its own motion in surge mode. Similarly, Figs. 4(c) and 4(d) show the results of diagonal terms (heave-heave) for non-dimensional added mass $\left({}^{22}a_{33}^{*}\right)$ and damping $\left({}^{22}b_{33}^{*}\right)$ of the body 2 (rectangular box) due to its own motion in heave mode. The present numerical results are compared with the numerical results of Dmitrieva and the experimental results of Oortmerssen (Dmitrieva, 1994). Similar to the previous figures i.e., Figs. 3(a)-3(d), the agreement between the calculated results are quite satisfactory, however the agreement with the experimental results present some deviations.

Fig. 5(a) presents the result of diagonal terms (surge-surge) for non-dimensional added mass $\left({}^{21}a_{11}^{*}\right)$ of body 2 (rectangular box) in surge mode due to the motion of body 1 (vertical cylinder) in surge mode. And also it shows the result of diagonal terms (surge-surge) for non-dimensional added mass $\left({}^{12}a_{11}^{*}\right)$ of body 1 (vertical cylinder) in surge mode due to the motion of body 2 (rectangular box) in surge mode. Similarly, Fig. 5(b) presents the result of diagonal terms (surge-surge) for non-dimensional damping $\left({}^{21}b_{11}^{*}\right)$ of body 2 (rectangular box) in surge mode due to the motion of body 1 (vertical cylinder) in surge mode and the result of diagonal terms (surge-surge) for non-dimensional damping $\left({}^{12}b_{11}^{*}\right)$ of body 1 (vertical cylinder) in surge mode due to the motion of body 2 (rectangular box) in surge mode. The present numerical results are compared with the numerical results of Dmitrieva (Dmitrieva, 1994). As can be seen from these figures, that the agreement between the calculated results are quite satisfactory. Moreover, Figs. 5(a) and 5(b) demonstrate that the symmetry relationships exist for hydrodynamic interaction coefficients.

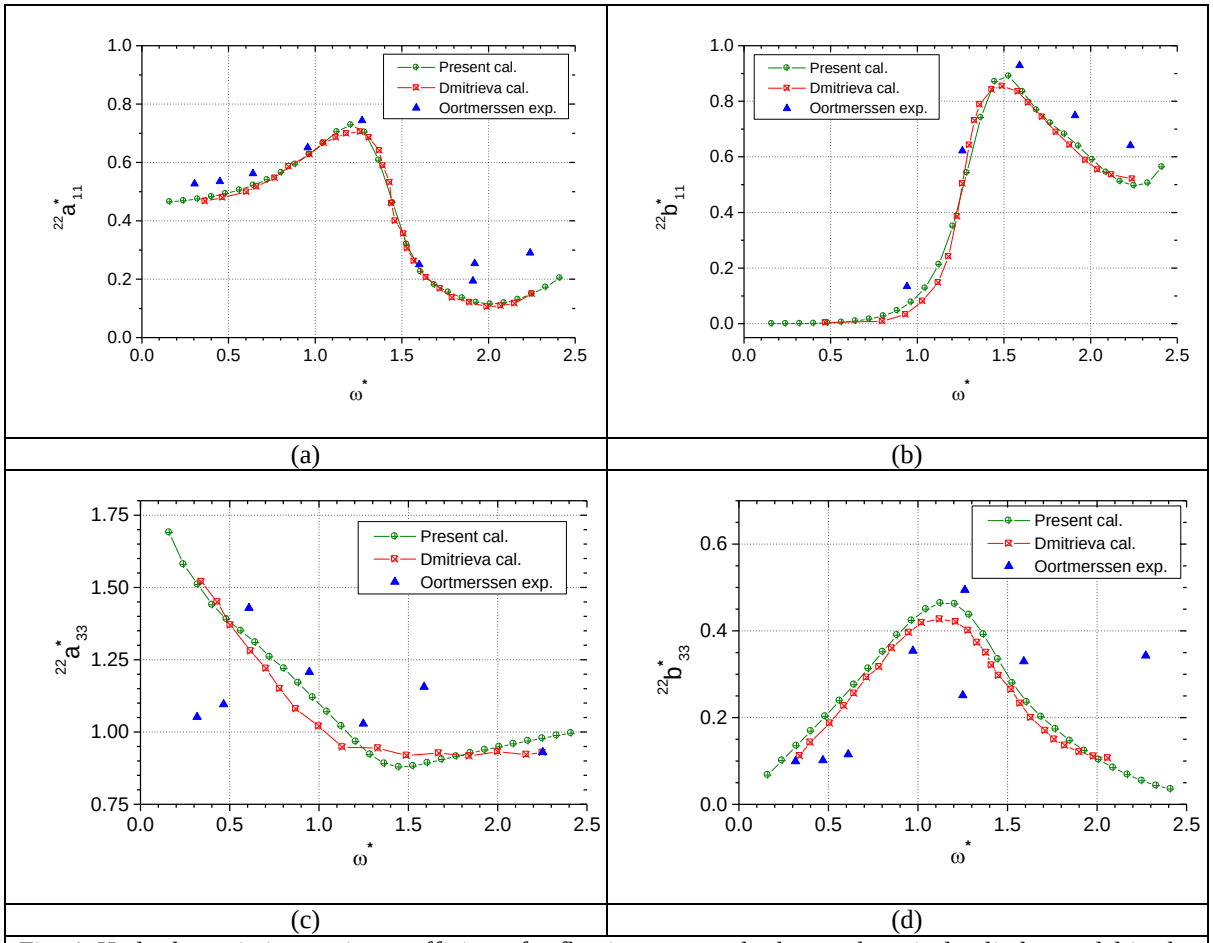

Fig. 4. Hydrodynamic interaction coefficients for floating rectangular box and vertical cylinder model in the side-by-side configuration

Fig. 5(c) present the result of coupling terms (surge-heave) for non-dimensional added mass $\left({}^{21}a_{13}^{*}\right)$ of body 2 (rectangular box) in surge mode due to the motion of body 1 (vertical cylinder) in heave mode and the coupling terms (heave-surge) for non-dimensional added mass $\left({}^{12}a_{31}^{*}\right)$ of body 1 (vertical cylinder) in heave mode due to the motion of body 2 (rectangular box) in surge mode. Fig. 5(d) present the result of coupling terms (surge-heave) for non-dimensional damping $\left({}^{21}b_{13}^{*}\right)$ of body 2 (rectangular box) in surge mode due to the motion of body 1 (vertical cylinder) in heave mode and the coupling terms (heave-surge) for non-dimensional added mass $\left({}^{12}b_{31}^{*}\right)$ of body 1 (vertical cylinder) in heave mode due to the motion of body 2 (rectangular box) in surge mode.

Fig. 5(e) present the result of coupling terms (heave-surge) for non-dimensional added mass $\left({}^{21}a_{31}^{*}\right)$ of body 2 (rectangular box) in heave mode due to the motion of body 1 (vertical cylinder) in surge mode and the coupling

terms (surge-heave) for non-dimensional added mass $\left({}^{12}a_{13}^{*}\right)$ of body 1 (vertical cylinder) in surge mode due to the motion of body 2 (rectangular box) in heave mode. Fig. 5(f) present the result of coupling terms (heave-surge) for non-dimensional damping $\left({}^{21}b_{31}^{*}\right)$ of body 2 (rectangular box) in heave mode due to the motion of body 1 (vertical cylinder) in surge mode and the coupling terms (surge-heave) for non-dimensional damping $\left({}^{12}b_{13}^{*}\right)$ of body 1 (vertical cylinder) in surge mode due to the motion of body 2 (rectangular box) in heave mode. The present numerical results are compared with the numerical results of Dmitrieva (Dmitrieva, 1994). It can be seen from these figures i.e., Figs. 5(c)~5(f), that the symmetry relationships are justified, and they also show an excellent agreement with the calculated results of Dmitrieva.

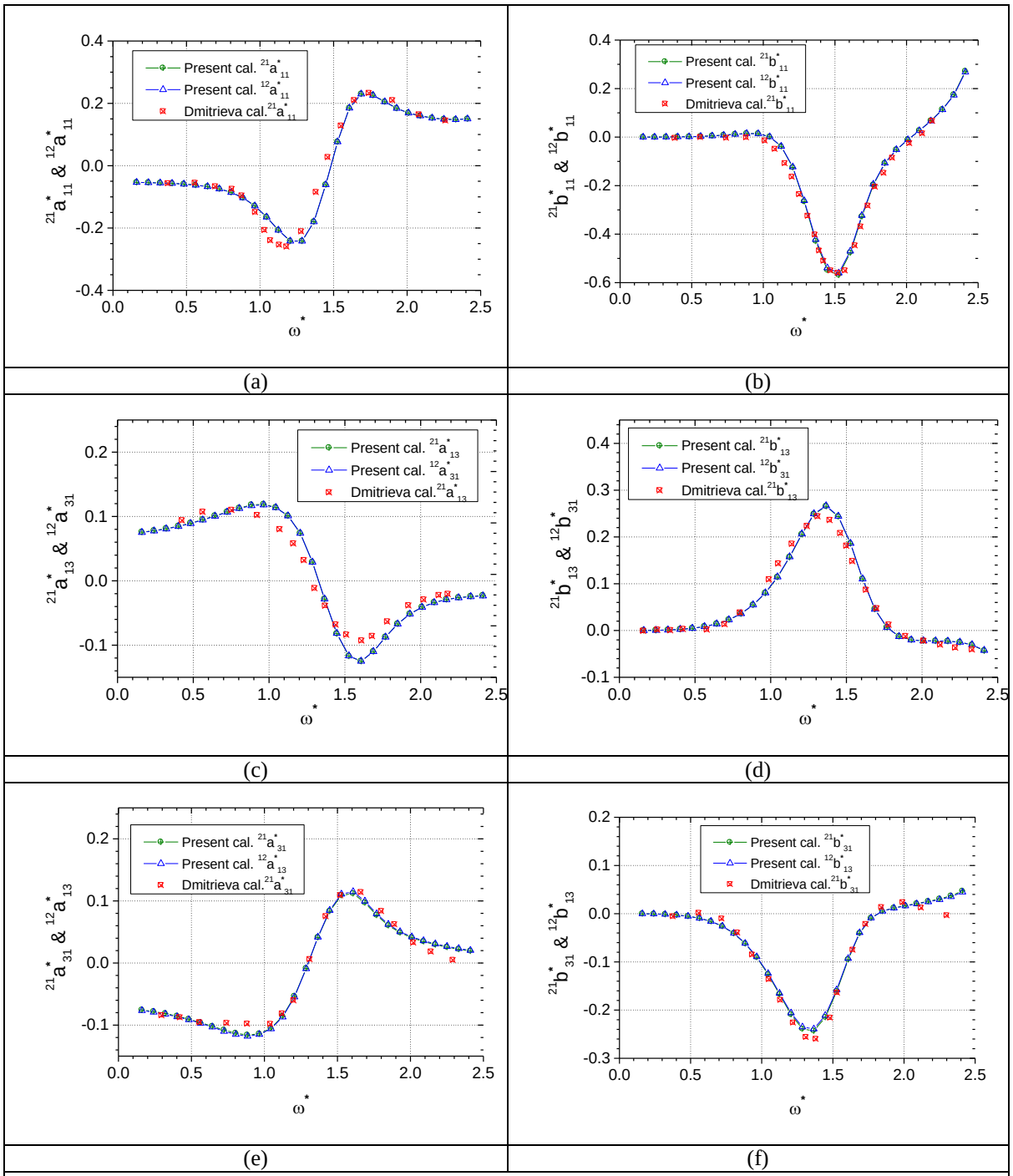

Fig. 5. Hydrodynamic interaction coefficients for floating rectangular box and vertical cylinder model in the side-by-side configuration

3.2 Two identical rectangular barges

The second model for multiple floating bodies is chosen as the two identical rectangular barges (Liang-yu. et al., 2014), floating in tandem configurations as shown in Fig. 6. For each identical rectangular barge, the length, breadth, and draft are 90 m, 27 m, and 4 m respectively, and each of their wetted surfaces is divided into 1083 panels. The water depth is considered 42 m.

For the tandem configuration of the two barges, the gap between these two floating bodies is varied as 9 m (10% of barge length), 18 m (20% of barge length), 27 m (30% of barge length) and 45 m (50% of barge length). For the wave heading angle in the tandem configuration as shown in Fig. 6., the weather side and lee side bodies are denoted as barge 2 and barge 1 respectively.

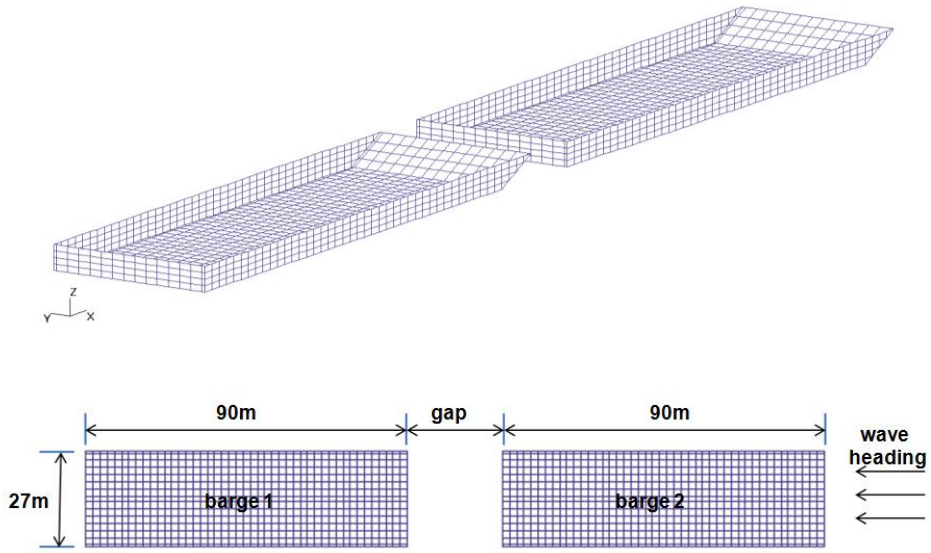

Fig. 6: 3-D mesh arrangements and plan view of two identical rectangular barges floating in waves with tandem configuration

The diagonal and coupling terms for surge, sway, heave, roll, pitch, and yaw mode of added mass are non-dimensionalized by dividing with $\rho\zeta_a\nabla$, $\rho\zeta_a\nabla l$ and $\rho\zeta_a\nabla l^2$. Similarly, the diagonal and coupling terms for damping are non-dimensionalized by dividing with $\rho\zeta_a\nabla\sqrt{g/l}$, $\rho\zeta_a\nabla l\sqrt{g/l}$ and $\rho\zeta_a\nabla l^2\sqrt{g/l}$. The numerical results are presented against wave frequency, which is non-dimensionalized by multiplying with $\sqrt{l/g}$, where the characteristics length l is 27.0 m.

The non-dimensional hydrodynamic interaction coefficients for various gap widths (10%, 20%, 30%, and 50% of the barge length) in the tandem configuration are compared with an isolated barge result as shown in Figures 7(a)-7(f). The figures display the results of diagonal terms−surge (11), heave (33) and pitch (55) added mass and damping of barge1 which is located at the lee side for the tandem arrangement. The shielding effect is also evident in the results when compared with the isolated barge results. The interaction effects are also nearly absent (weak) for the lower frequency range($\omega^* < 1$). The surge and pitch added mass results as shown in Figs. 7(a) and 7(e) display gradual fluctuations at a higher frequency range although the gap width effect is not clear. Almost no interaction effects are observed in the heave added mass results as can be seen in Fig. 7(c). The surge, heave and pitch damping results as presented in Figs. 7(b), 7(d) and 7(f) display spikes at higher frequency range ($\omega^* > 2$) for various gaps except for the 10% gap width where the spike is not noticeable. As the gap width between the two barges increases, the resonance phenomenon in the gap shifts from the pumping mode to the sloshing mode (Molin, 2001). This may be attributed to the presence of multiple spikes for wider gap width.

Finally, Figs. 8(a)~8(d) display the results considering various gap widths (10%, 20%, 30%, and 50% of the barge length) in the tandem configuration of coupling terms for added mass and damping of $({}^{12}a_{11}^{*}, {}^{21}a_{11}^{*})$, $({}^{12}a_{35}^{*}, {}^{21}a_{53}^{*})$, $({}^{12}b_{51}^{*}, {}^{21}b_{15}^{*})$ and $({}^{12}a_{55}^{*}, {}^{21}a_{55}^{*})$, in which sharp spikes are nearly absent although the gap widths affect the magnitudes of the smooth curves. The numerical results exhibit that symmetry relationships exist for hydrodynamic interaction coefficients.

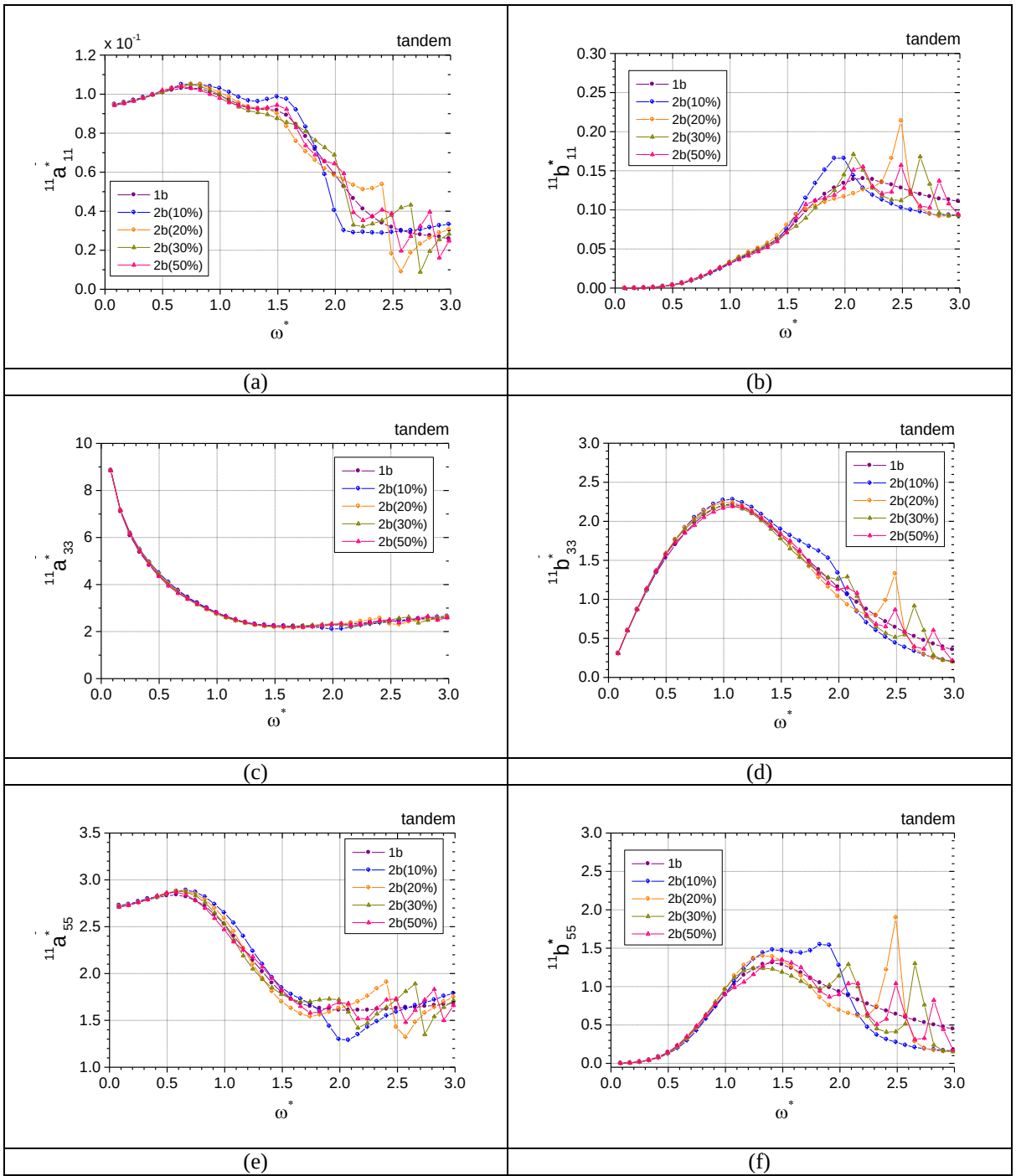

Figure 7. Non-dimensional hydrodynamic interaction coefficients (added mass and damping) of diagonal terms surge(11), heave (33) and pitch(55) of barge1(lee side) for various gap widths in tandem configurations of rectangular floating barges

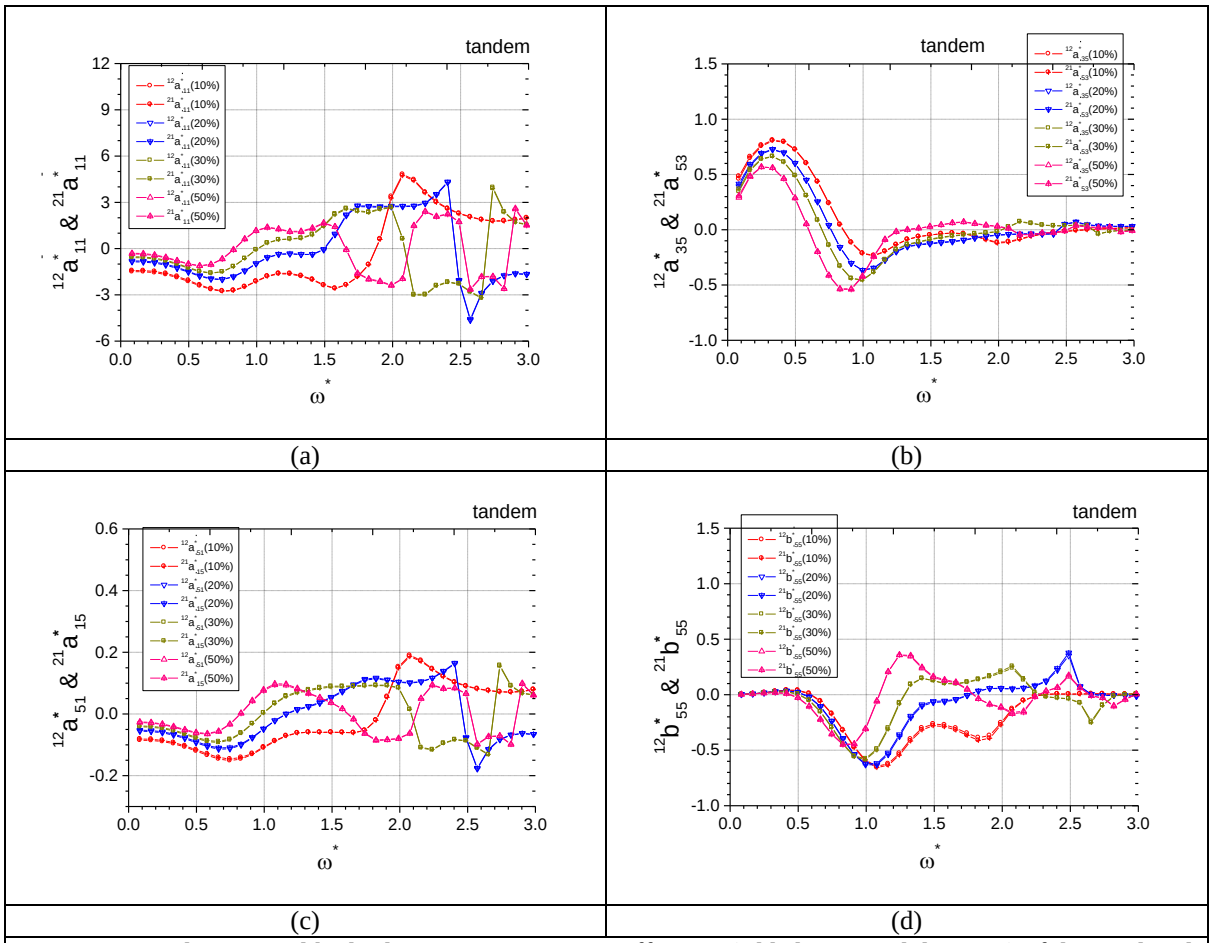

Figure 8. Non-dimensional hydrodynamic interaction coefficients (added mass and damping) of diagonal and coupling terms surge(11), heave (33) and pitch(55) for various gap widths in tandem configurations of rectangular floating barges

3.3 Resonant mode and hydrodynamic interaction coefficients

Molin (2001) proposed an analytical solution to estimate the resonant frequency up to the n-th order. This approach considers the 3-D effect by incorporating the length(l), width(b) and draft(h) of the gap between the floating bodies. The non-dimensional resonant frequencies ($\omega^*_{n0} = \omega_{n0}\sqrt{l/g}$) can be estimated by using Dirichlet function as

$$\omega_{n0}^2 \simeq g\lambda_n \frac{1 + J_{Dn0}\tanh\lambda_n h}{J_{Dn0} + \tanh\lambda_n h} \tag{9}$$

$$J_{Dn0} = \frac{2}{n\pi^2 r}\left\{\int_0^1 \frac{r^2}{u^2\sqrt{u^2+r^2}}\left[1+2u+(u-1)\cos(n\pi u) - \frac{3}{n\pi}\sin(n\pi u)\right]du - \frac{1}{\sin\theta_0} + 1 + 2r\ln\frac{1+\cos\theta_0}{1-\cos\theta_0}\right\} \tag{10}$$

Using Molin's approach, the first four gap resonant modes are calculated for various gap widths as presented in Table 2. It is thus evident that the gap widths might play a significant role in the simulation results, although correlating the wave frequency location of spikes in the numerical results with the estimated resonance frequencies is not a straightforward task.

Table2. The calculated resonant mode

		Gap width			
Resonant mode	$\omega^*_{n0} = \omega_{n0}\sqrt{l/g}$	10%	20%	30%	50%
		ω^*_{n0}	ω^*_{n0}	ω^*_{n0}	ω^*_{n0}
	1st	1.82	1.87	1.83	1.75
	2nd	2.50	2.58	2.60	2.59
	3rd	3.06	3.11	3.12	3.13
	4th	3.54	3.56	3.57	3.58

4. Conclusions

The 3-D source distribution method has been applied to study the characteristics of hydrodynamic interaction coefficients of added mass and damping for two closely floating identical rectangular barges of tandem configurations in regular waves. Hydrodynamic interaction effects are absent at the lower frequency range. In the higher frequency range with wider gap widths, the added mass results display sharp fluctuation with increase in magnitude and the spikes are evident for damping results. The shielding effect is evident in the results while comparing with the isolated barge results. The location of oscillating local peaks may be correlated with the estimated resonant modes and the gap widths might play a significant role in the simulation results. The symmetry relationship exists for the hydrodynamic interaction coefficients of added mass and damping for floating multi-body problem.

References

Ali, M. T. (2021): A numerical investigation on hydrodynamic interaction coefficients for a group of truncated composite cylinders floating in waves, Proceeding of the ASME 40th International Conference on Ocean, Offshore and Arctic Engineering, OMAE2021-63037, Virtual, Online. https://doi.org/10.1115/OMAE2021-63037

Ali, M. T. (2020): A numerical investigation on hydrodynamic interaction coefficients for multiple freely floating bodies in waves, Proceeding of the ASME 39th International Conference on Ocean, Offshore and Arctic Engineering, OMAE2020-19315, Virtual, Online. https://doi.org/10.1115/OMAE2020-19315

Chen, M., Guo, H., Wang, R., Tao, R. and Cheng, N. (2021): Effects of gap resonance on the hydrodynamics and dynamics of a multi-module floating system with narrow gaps, Journal of Marine Science and Engineering, Vol. 9, 1256. https://doi.org/10.3390/jmse9111256

Dinoi, P. (2016): Analysis of wave resonant effects in-between offshore vessels arranged side-by-side, Ph. D. Thesis, Technical University of Madrid. https://doi.org/10.20868/UPM.thesis.43593

Dmitrieva, I. N. (1994): Numerical investigations of hydrodynamic coefficients and hydrodynamic interaction between two floating structures in waves, Ship Hydrodynamic Laboratory, Delft University of Technology, Report No. 1018.

Ghafari, H., Ketabdari, M., Ghassemi, H. and Homayoun, E. (2019): Numerical study on the hydrodynamic interaction between two floating platforms in Caspian Sea environmental conditions, Ocean Engineering, Vol.188, 106273. https://doi.org/10.1016/j.oceaneng.2019.106273

Li, B. (2020): Multi-body hydrodynamic resonance and shielding effect of vessels parallel and nonparallel side-by-side, Ocean Engineering, Vol. 218, 108188. https://doi.org/10.1016/j.oceaneng.2020.108188

Liang-yu, X. U., Jian-min, Y., Xin, L.I. and Xin, X. U. (2014): Numerical and experimental study on hydrodynamic interactions between two side-by-side barges in close proximity, Journal of Ship Mechanics, Vol. 18, No. 3, pp. 248-261. http://dx.doi.org/10.3969/j.issn.1007-7294.2014.03.005

Molin, B. (2001): On the piston and sloshing modes in moonpools, Journal of Fluid Mechanics, Vol. 430, pp. 27-50. https://doi.org/10.1017/S0022112000002871

Sun, L., Eatock Taylor, R., and Choo, Y. S. (2012): Multi-body dynamic analysis of float-over installations, Ocean Engineering, Vol. 51, pp. 1-15. https://doi.org/10.1016/j.oceaneng.2012.05.017

Van Oortmerssen, G. (1979): Hydrodynamic interaction between two structures of floating in waves, Proceedings of 2nd International Conference of Behavior of Offshore Structures, Vol. 1, pp. 339-356.